

General Disclaimer

One or more of the Following Statements may affect this Document

- This document has been reproduced from the best copy furnished by the organizational source. It is being released in the interest of making available as much information as possible.
- This document may contain data, which exceeds the sheet parameters. It was furnished in this condition by the organizational source and is the best copy available.
- This document may contain tone-on-tone or color graphs, charts and/or pictures, which have been reproduced in black and white.
- This document is paginated as submitted by the original source.
- Portions of this document are not fully legible due to the historical nature of some of the material. However, it is the best reproduction available from the original submission.

Tmx-71298

MEAN SEA LEVEL DETERMINATION FROM SATELLITE ALTIMETRY

(NASA-TM-X-71298) MEAN SEA LEVEL N77-21530
DETERMINATION FROM SATELLITE ALTIMETRY
(NASA) 28 p EC A03/MF A01 CACL 05B
G3/43 Unclass
25822

W.D. KAHN
B.B. AGRAWAL
R.D. BROWN

MARCH 1977



GODDARD SPACE FLIGHT CENTER
GREENBELT, MARYLAND



**X-921-77-41
PREPRINT**

**MEAN SEA LEVEL DETERMINATION FROM
SATELLITE ALTIMETRY**

W. D. Kahn

Goddard Space Flight Center

B. B. Agrawal

R. D. Brown

Computer Sciences Corporation

March 1977

GODDARD SPACE FLIGHT CENTER

Greenbelt, Maryland

**MEAN SEA LEVEL DETERMINATION FROM
SATELLITE ALTIMETRY**

W. D. Kahn

Goddard Space Flight Center

B. B. Agrawal

R. D. Brown

Computer Sciences Corporation

ABSTRACT

The primary experiment on the Geodynamics Experimental Ocean Satellite-3 (GEOS-3) is the radar altimeter. This experiment's major objective is to demonstrate the utility of measuring the geometry of the ocean surface, i.e. the geoid. Results obtained from this experiment so far indicate that the planned objectives of measuring the topography of the ocean surface with an absolute accuracy of ± 5 meters can be met and perhaps exceeded.

The GEOS-3 satellite altimeter measurements have an instrument precision in the range of ± 25 cm to ± 50 cm when the altimeter is operating in the "short pulse" mode.

After one year's operations of the altimeter, data from over 5,000 altimeter passes have been collected. With the mathematical models developed and the altimeter data presently available, mapping of local areas of ocean topography has been realized to the planned accuracy levels and better. This paper presents the basic data processing methods employed and some interesting results achieved with the early data. Plots of mean surface heights as inferred by the altimeter measurements are compared with a detailed $1^{\circ} \times 1^{\circ}$ gravimetric geoid.

CONTENTS

	Page
INTRODUCTION	4
MATHEMATICAL MODELS:	6
GEOD PROPERTIES	6
Undulation Amplitude	7
MEASUREMENT GEOMETRY AND MATHEMATICAL MODELS . .	9
Results	16
SUMMARY	18
ACKNOWLEDGEMENTS	18
REFERENCES	18

MEAN SEA LEVEL DETERMINATION FROM SATELLITE ALTIMETRY

INTRODUCTION

The GEOS-3 altimeter experiment objectives are (1) to determine the feasibility and utility of a spaceborne altimeter to map the ocean geoid with absolute height-resolution of ± 5 meters and a relative height precision of ± 1 to ± 2 meters, (2) to determine the feasibility of measuring the deflections of the vertical at sea, (3) to determine the feasibility of measuring wave height and (4) to contribute to technology leading to a future operational satellite altimeter system with a 10 cm measurement capability. This paper addresses objective 1 above.

Satellite tracking contributions to the determination of the current ocean geoid have a spatial resolution corresponding to a half wavelength of approximately 11 to 15 degrees (1250 to 1650 km). Although the addition of surface gravity permits local representations with finer resolution, in the 1-to-5 degree (110-to-550 km) range these data are available over only about 50 percent of the ocean surface.

The GEOS-3 altimeter has demonstrated the capability to determine the fine structure of the mean sea surface. When this instrument is operating in the short pulse mode a measurement is produced every 4 km along the satellite subtrack. With this resolution capability it will be possible to describe sea

surface topography to a detail of less than 1° , depending on the degree of data smoothing used and the spacing between subtracks.

The GEOS-3 altimeter system therefore fills the gap in data coverage and also provides valuable independent knowledge where data now exist.

When the altimeter data are calibrated and corrected (e. g. , for sea state, ocean tides, and other effects) the data constitute measures of the distance between the GEOS-3 satellite and the mean sea level, (MSL) or geoid surface. Knowledge of the satellite orbital altitude relative to the reference ellipsoid will then permit the determination of the geoid. The chief problem encountered thus far is the accurate determination of the orbital altitude for GEOS-3. This paper will primarily discuss the altimeter measurement geometry and the mathematical procedure used to correct orbit errors in the GEOS-3 altimeter data. Intercomparisons between processed altimeter sea height profiles and independent geoid estimates will be shown.

MATHEMATICAL MODELS:

GEOID PROPERTIES

The geoid is an imaginary surface, a particular equipotential surface of the geopotential field. This surface is nearly spherical, with a slight flattening at the poles and a pear-shaped bulge in the southern hemisphere. Smaller scale deviations from the spherical surface can be deduced from the magnitudes of the higher order terms in a spherical harmonic model of the geopotential; this reveals a nonuniform distribution of surface roughness with surface relief on the order of one part in ten thousand. The geoid is approximated closely by a real surface, the sea surface, in ocean areas. The sea surface would conform exactly to the geoid in the absence of currents, tides, and weather-related phenomena (Reference 1). The exact shape of this mean-sea-level (MSL) or marine geoid surface is dictated by the spatial variations in the gravitational potential of the rotating earth. Its shape is important for this study because ideally it is the sea surface that is defined by the altimeter measurements.

The properties of the MSL surface are represented by the geoid undulation, which is the deviation of the geoid from the best fitting ellipsoid as measured along the ellipsoid normal.

Undulation Amplitude

Because the magnitude of the geoid surface relief is very small relative to the earth's radius, a reference surface that closely approximates the geoid is customarily utilized to avoid working with small differences in large numbers. This reference surface is usually chosen as the rotationally symmetrical ellipsoid that best fits the geoid, in a least-squares sense, to the accuracy that the geoid is presently known. This surface plays another role in that it represents an equipotential surface of the "normal" potential of the geopotential field. The additional factor (the "disturbing" potential) needed to fully describe the geopotential is thus made small.

The geopotential may be described in geocentric earth-fixed coordinates as

$$W(X, Y, Z) = U(X, Y, Z) + T(X, Y, Z) \quad (1)$$

where

W = the geopotential

U = the normal potential

T = the disturbing potential at the point (X, Y, Z).

To evaluate the magnitude of geoid undulations, one compares the geoid (described by a particular equipotential surface)

$$W(X, Y, Z) = W_0 \quad (2)$$

with the reference ellipsoid

$$U(X, Y, Z) = U_0 \quad (3)$$

of the same potential

$$U_0 = W_0 \quad (4)$$

Following Heiskanen and Moritz (Reference 2) and referring to Figure 1, a point P on the geoid is projected along the ellipsoid normal onto point Q on the ellipsoid. This distance PQ, denoted by N, is called the geoidal undulation at P.

One may approximate the value of the normal potential U at P by a linear relation

$$U_P = U_Q + \left(\frac{\partial U}{\partial \hat{n}} \right)_Q N \triangleq U_Q - \gamma_Q N \quad (5)$$

where γ_Q is the acceleration of gravity calculated at the ellipsoid surface.

Since by definition

$$W_P = U_P + T_P \quad (6)$$

and since

$$W_P = W_0 = U_Q \quad (7)$$

we find by substituting Equations (7) and (6) into (5) that the geoidal undulation is given by

$$N = \frac{T_P}{\gamma_Q} \quad (8)$$

MEASUREMENT GEOMETRY AND MATHEMATICAL MODELS

The altimeter measurement is nominally the shortest distance between the satellite and the sea surface. It is along the normal to the sea surface that passes through the satellite. The satellite altimeter antenna is controlled to point along the local vertical at satellite altitude. Because equipotential surfaces at satellite altitude are even closer approximations to an ellipsoid than is the geoid, this local vertical can also be assumed to be the normal to an ellipsoidal surface. However, this normal is not generally the same as the reference ellipsoid normal due to curvature of the gradient of the normal potential. The use of an antenna beamwidth of 1 or 2° insures that the first return from the sea surface is within the beamwidth of the antenna. Assuming that the measurement is made along the ellipsoid normal at S', the factors that influence the error in the measured altitude are represented in Figure 2.

Figure 2 shows the beam pattern of a spacecraft-borne altimeter sensor system that is oriented in the direction of the gravity acceleration vector (\vec{g}) at the satellite. The height of the satellite is measured in the direction of shortest

signal echo, which is very close to the local normal, \hat{n} , to the geoid (i. e. the direction of line segment SP), especially over ocean areas.

Ideally, the satellite altitude at P should be calculated along the line from P to the satellite, of distance h_a . However, the location of point P is not known initially, so approximate techniques are used. Although the quantity N' is not exactly equal to N , nor colinear with the SP line segment, the height of the satellite above the ellipsoid may be approximated initially as

$$h_a \cong h - N' - \delta h_s - \Delta h' \quad (9)$$

where

h = magnitude of \vec{h} , S/C altitude above the reference ellipsoid at S'

h_a = S/C altitude above the geoid at P

N' = geoid height above reference ellipsoid

δh_s = deviation of sea surface from geoid

$\Delta h'$ = systematic errors in altimeter measurement,

e. g. , refraction, antenna offset, timing, etc.

This error sources that affect the altimeter measurement fall into three categories: (1) those that result from orbit uncertainty; (2) those that result from deviation between the measured surface and the true geoid; and (3) those that affect the measurement accuracy itself, i. e. , instrument errors and propagation effects. The functional dependence of the error sources on the

altimeter measurement is given by (Reference 3)

$$h_a = h(\vec{E}, t) - N'(\vec{G}) - \delta h_s(\vec{\tau}, \vec{s}, \phi, \lambda, t) - \Delta h'(\vec{m}, \phi, \lambda, t) \quad (10)$$

where

- \vec{E} = orbit parameters and orbit dependent terms (radiation pressure, drag, etc.)
- t = time of altimeter measurement
- \vec{G} = vector of geopotential coefficients
- $\vec{\tau}$ = vector of tidal error model coefficients
- \vec{s} = vector of local sea-surface biases (i. e. , currents, storm surges, wind waves . . .)
- \vec{m} = vector of altimeter measurement error coefficients
- ϕ = latitude
- λ = longitude

or in general

$$h_a = h_a(\vec{E}, \vec{G}, \vec{\tau}, \vec{s}, \vec{m}, \phi, \lambda, t) \quad (11)$$

The dominant error source is that due to uncertainty in the orbit.

The instantaneous sea surface generally is within a meter or two of the geoid (Reference 1), but such deviations cannot be neglected if an altimeter accuracy of 1 meter or less is desired. Similarly the measurement errors are neglected, being of the order of 1 m.

Comparing the altimeter measurement, h'_a with altitude calculated from the satellite's orbit h_a , the measurement residual Δh_a is formed.

$$\Delta h_a = h'_a - h_a \quad (12)$$

The computation of altitude from an orbit based on independent tracking data sets has been noted to produce residuals which exhibit systematic offset or trends. This systematic offset, due in large measure to orbit uncertainty, is reduced by differential correction of the orbit using altimeter data. The resultant residuals in satellite altitude exhibit almost complete freedom from systematic errors.

The data processing procedure for accomplishing this removal of orbit uncertainty effects is as follows. The high rate (10/sec or 100/sec) binary format altimeter measurement data is processed in the GEODYN Program, a general purpose orbit determination program in use at the NASA Goddard Space Flight Center, where a tidal correction is applied and the data is converted to geoid heights. The program has been modified to permit the differential correction of orbital elements from altimeter data. This process can be used to converge the altimetric geoid heights on a profile through a reference geopotential level surface, in this case, the Goddard Earth Model-7 (GEM-7) geoid (Reference 4). The adjusted orbit parameters serve merely as accommodation coefficients in this process and effect a removal of bias, trend, and

long wavelength curvature from the relatively short arcs of altimeter data. While all six orbit parameters are adjusted, significant changes (greater than the standard deviation of the estimate) usually only occur in the orbit semi major axis, eccentricity and the true anomaly. Significant changes in the remaining Keplerian parameters may also occur for the longer arcs.

This process minimizes the square of deviations of the altimetric geoid heights from the GEM-7 geoid, as is shown in the following development. The expected altitude of the spacecraft may be written (neglecting sea surface effects and altimeter system errors) as

$$h_a(t) = h(\vec{e}, t) - N'(\vec{G}) \quad (13)$$

where h is the satellite height above the reference ellipsoid as a function of the state vector of the satellite \vec{e} , and N' is the geoid undulation as a function of geopotential parameters \vec{G} . The actual altitude measurement $h'_a(t)$ is related to the expected altitude (with suitable differential corrections to the parameters) by

$$h'_a(t) - h_a(t) = \frac{\partial h}{\partial \vec{e}} \Delta \vec{e} - \frac{\partial N'}{\partial \vec{G}} \Delta \vec{G} + \delta \quad (14)$$

where δ is the vector of unmodelled errors in the altimeter measurement. Subsequent formation of normal equations solving for corrections to the parameters on the right hand side of equation 14 will yield a least squares best fit of h_a to h'_a .

We may rewrite (14) in terms of geoid undulations by substituting (13) into (14) and rearranging

$$N'(\vec{G}) = h(\vec{e}, t) - h'_a(t) + \frac{\partial h}{\partial \vec{e}} \Delta \vec{e} - \frac{\partial N'}{\partial G'} \Delta G' + \delta \quad (15)$$

Due to the near colinearity and similarity of dimension between h_a and N' , we may consider (15) to be an observation equation for geoid undulations. If we desire to obtain a least squares fit between these altimetric geoid undulation observations and the GEM-7 geoid undulations, we need only substitute N' (GEM-7, t) for the left-hand side of (15) and adjust suitable parameters on the right hand side. To evaluate the short wavelength differences between the altimetric geoid and the GEM-7 geoid, adjustment of \vec{e} alone is indicated, since these parameters affect only the relatively long wavelength behavior of the altimetric geoid data record. Therefore, we adopt the following equation

$$N'(\text{GEM-7}, t) - h(\vec{e}, t) + h'_a(t) = \frac{\partial h}{\partial \vec{e}} \Delta \vec{e} + \delta \quad (16)$$

as our observation equation, form the corresponding normal equation, adjust the orbit parameters in an iterative differential correction process, and

obtain a converged set of altimetric geoid heights

$$\bar{N}(t) = h(\vec{e}_c, t) - h'_a(t) \quad (17)$$

which are a least squares fit to the GEM-7 geoid heights $N(\text{GEM-7}, t)$. The adjusted orbit parameters \vec{e}_c serve only to effect the fitting process and are of no intrinsic significance. Note that equation (16) is exactly equivalent to equation (14). We have simply transformed our observations from altitudes to geoid heights.

An example of the results of this process is shown in Figure 3 for pass number 254. This process removes all bias, linear drift, and long wavelength phenomena from the altimetric geoid heights, including possible long wavelength geoid information. Since GEM-7 is complete only through degree and order 16, with a few terms as high as degree 30, one expects the converged geoid heights spectrum to contain geoid information and altimeter noise of wavelength shorter than 2500 km. One must be careful in attempting this convergence with passes shorter than 2500 km, because aliasing with the long wavelength terms in GEM-7 may cause erroneous removal of information of shorter wavelengths.

Implicit in this process is the assumption that the GEM-7 geoid is an accurate representation of the long wavelength effects of the geoid, which may or may not be true. In any case, it is a simple matter to convert these converged

geoid heights to another more accurate analytical model reference surface when the need arises.

Results

The GEOS-3 altimeter has consistently demonstrated the ability to detect true sea surface topography. Figure 4a represents an altimeter pass going from the northeast towards the southwest in the western North Atlantic. The satellite passes over the well known Puerto Rico trench. This feature is clearly indicated in the sea surface height profile as generated from altimeter data (Figure 4b). In this same figure very close agreement is seen between the GEOS-3 sea surface height profile and the $1^{\circ} \times 1^{\circ}$ detailed gravimetric geoid. In figure 4c, agreement between the GEOS-3 sea surface height profile and bathymetric measurements is also demonstrated.

Other geographic areas traversed by GEOS-3 also exemplify the aforementioned agreement between the altimeter measured sea surface topography and the $1^{\circ} \times 1^{\circ}$ detailed geoid. Figure 5 shows the close comparison between the altimeter measured sea surface height profile and the $1^{\circ} \times 1^{\circ}$ detailed geoid for the mid-Atlantic ridge region.

Figure 6 shows the fine structure differences between GEOS-3 altimeter measured sea surface height profile and the detailed gravimetric geoid.

Of particular interest is the Aleutian trench area. There is close agreement

between the altimeter measured sea surface height profile and the $1^\circ \times 1^\circ$ detailed geoid except in the Aleutian trench area where the difference is as high as 10 meters. This difference reflects the lack of surface gravity data of sufficient accuracy and densification in that region. It suggests that altimetry can make a significant contribution to more accurate geoid/geopotential modeling.

Figure 7 is an altimeter profile of both sea and land topography which clearly shows the variation in height between the ocean area and land. Most spectacular are the signatures of lakes Erie, Huron, and Superior. The variation between sea level and the height measured by the GEOS-3 altimeter of these Great Lakes closely correlates with topographic survey measurements. The large excursions in "sea surface height" are, as one would expect, due largely to the changes in received signal strength as the altimeter traverses areas of changing surface reflectivity.

Finally, Figure 8 shows the GEOS-3 altimeter sea surface height profile over the Formosa Strait, in the vicinity of the boundary between the Philippine and China tectonic plates. The fine structure of the measured altimeter height profile does not agree with the detailed geoid for this area, again due to the lack of surface gravity data of sufficient accuracy and densification. It should be noted, that the altimeter depicts a geoid depression which is not

associated with a bathymetric feature such as a trench, but which is recognized as a subduction zone between the above mentioned plates.

SUMMARY

Data from selected GEOS-3 altimeter passes have demonstrated the ability to represent precisely the fine structure of the sea surface. Close agreement has been shown between the measured sea height profile, the detailed geoid, bathymetry, and the structure of tectonic plates. Future application of altimeter measurements will be to determining a detailed global geoid with an absolute vertical accuracy of better than 5 meters and a horizontal spatial resolution of better than 500 km.

ACKNOWLEDGEMENTS

The authors are greatly indebted to the GEOS-3 project scientist, R. H. Stanley of NASA/Wallops station for providing invaluable hints for processing and interpreting the GEOS-3 altimeter data.

REFERENCES

1. New York University School of Engineering and Science, Department of Meteorology and Oceanography, Report on Contract N62306-1589, U. S. Naval Oceanographic Office, Radar Altimetry from a Spacecraft and its Potential Applications to Geodesy and Oceanography, J. A. Greenwood, et al., May 1967.
2. Heiskanen, W. A. and H. Moritz, Physical Geodesy, W. H. Freeman and Co., 1967.
3. Brown, R. D. and R. J. Fury, Computer Sciences Corporation, "Determination of the Geoid from Satellite Altimeter Data," NASA Goddard Space Flight Center X-550-72-268, September 1972.
4. Wagner, C. A., F. J. Lerch, J. E. Brownd, and J. A. Richardson, "Improvement in the Geopotential From Satellite and Surface Data (GEM-7 and -8)" NASA Goddard Space Flight Center, X-921-76-20, January 1976.

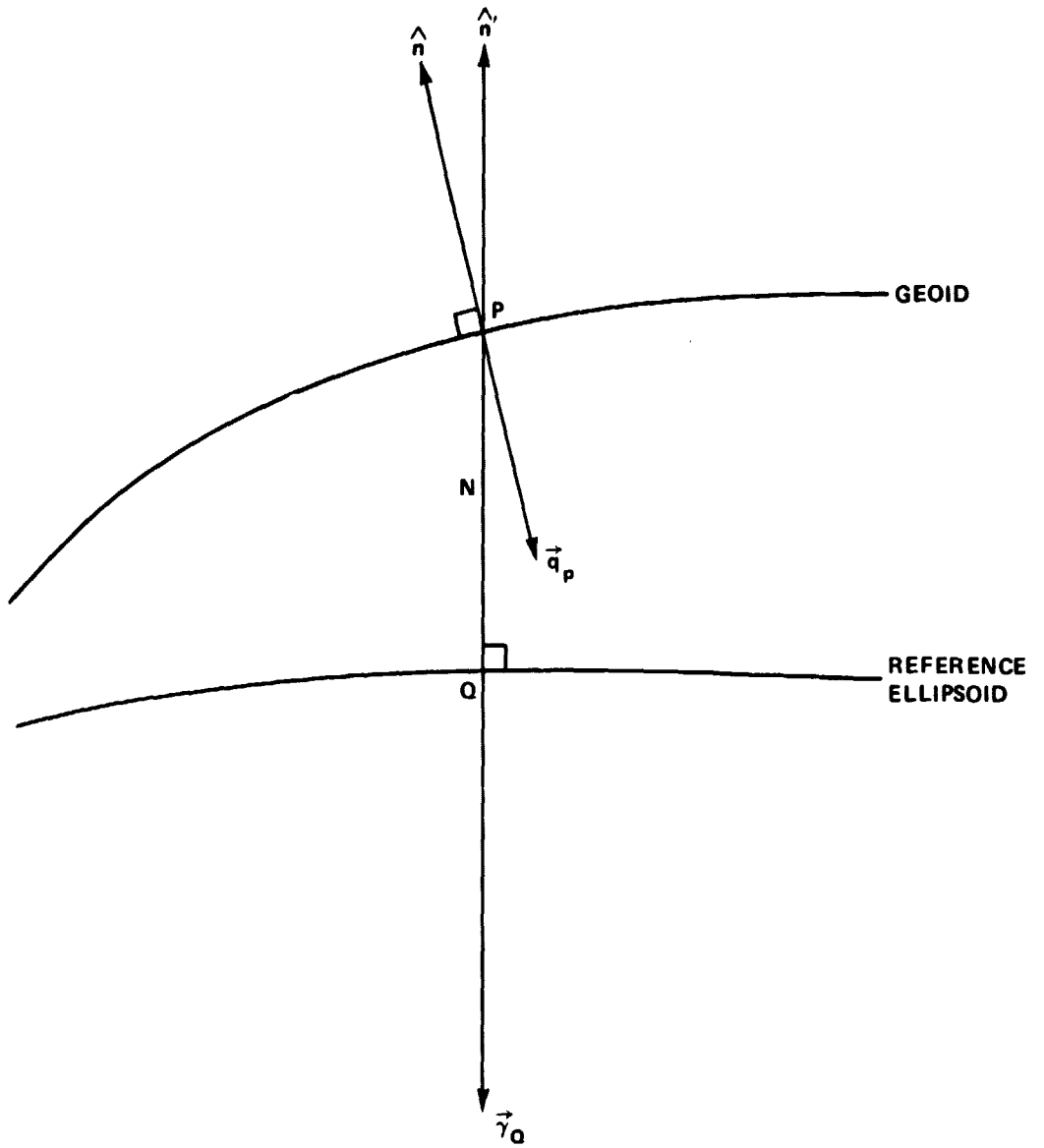


Figure 1 Geoid and Reference Ellipsoid

PRECEDING PAGE BLANK NOT FILMED

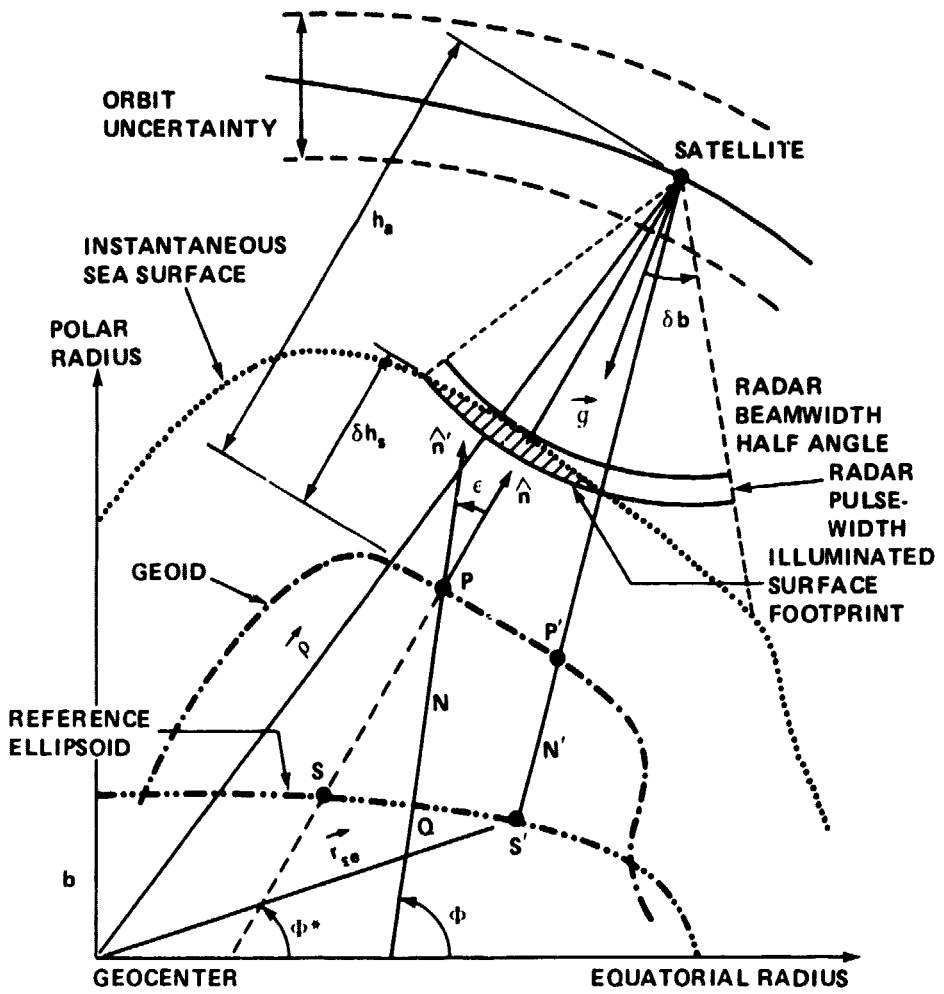
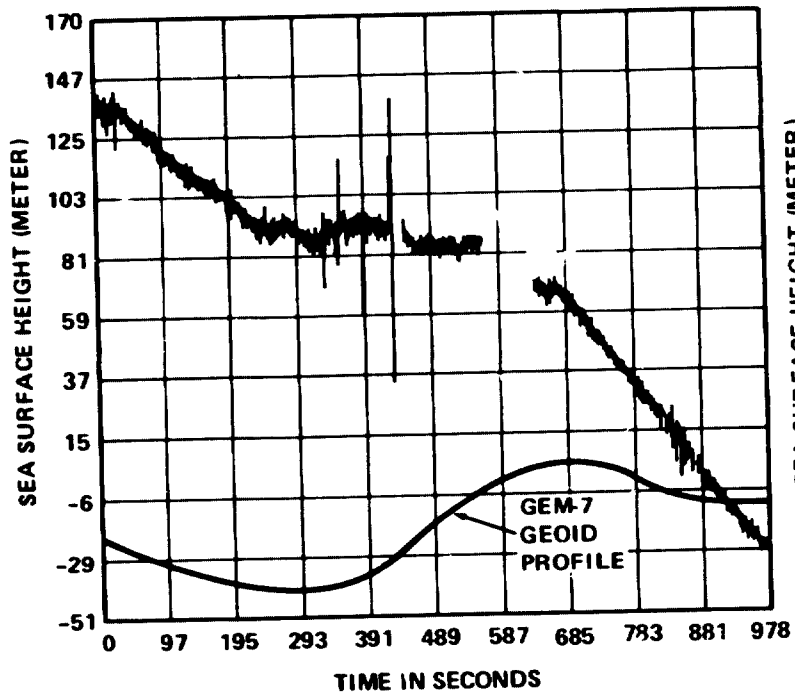
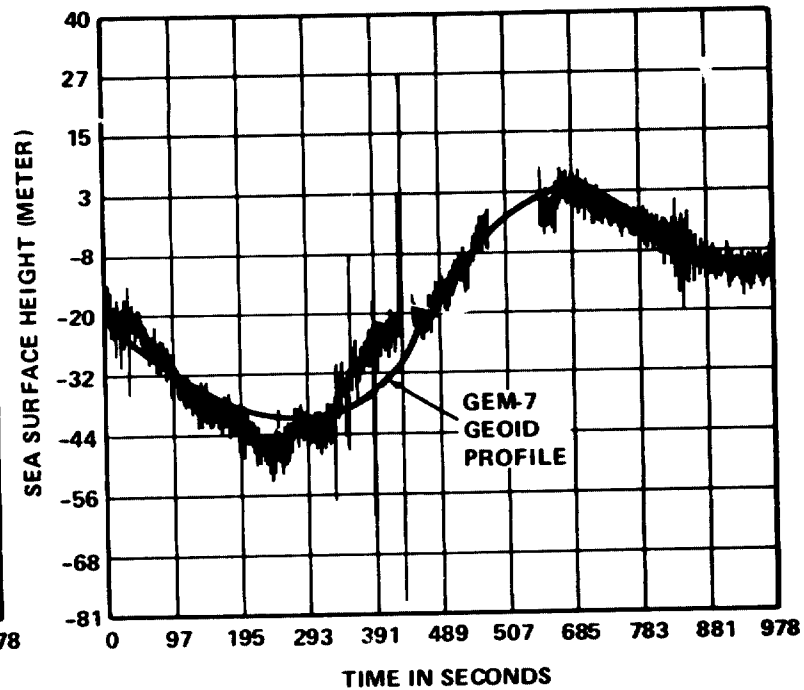


Figure 2 Altimeter Measurement Geometry



(A) BEFORE CONVERGENCE



(B) AFTER CONVERGENCE

Figure 3 Convergence of Pass 254 on the GEM-7 Geoid

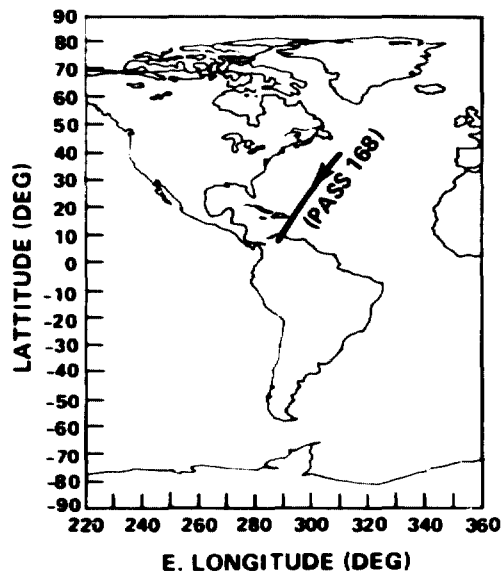


FIGURE 4(a) GEOS-3 ORBIT SUBTRACK FOR ALTIMETER PASS 168

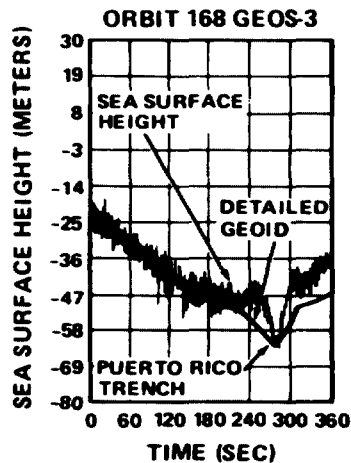


FIGURE 4(b) SEA SURFACE HEIGHT COMPARISON WITH $1^{\circ} \times 1^{\circ}$ GSFC DETAILED GEOID. TIME FROM APRIL 21, 1975 20H 59M 15S

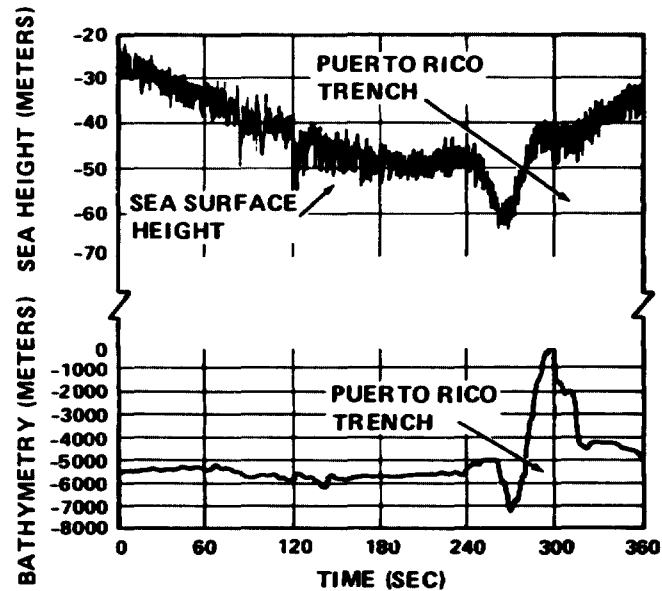


FIGURE 4(c) GEOS-3 SEA SURFACE HEIGHT PROFILE COMPARED WITH BATHYMETRY FOR PASS 168

Figure 4 GEOS-3 Sea Surface Height Profile in the Atlantic Area Compared with the GSFC $1^{\circ} \times 1^{\circ}$ Detailed Geoid

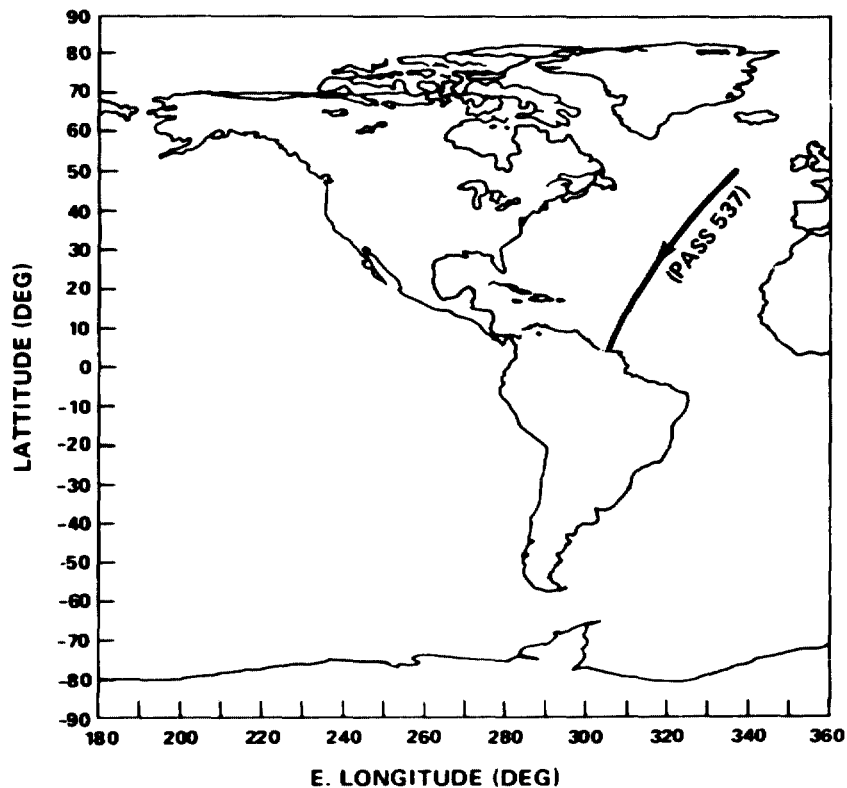


FIGURE 5(a) GEOS-3 ORBIT SUBTRACK FOR ALTIMETER PASS 537

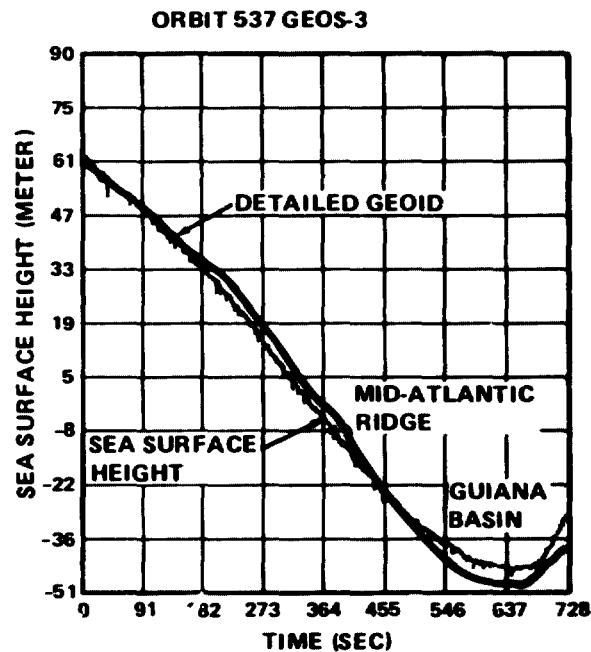


FIGURE 5(b) SEA SURFACE HEIGHT COMPARISON WITH 1°x1° GSFC DETAILED GEOID. TIME FROM MAY 17, 1975 22H 54M56S

Figure 5 GEOS-3 Sea Surface Height Profile in the Atlantic Area Compared with the GSFC 1° x 1° Detailed Geoid

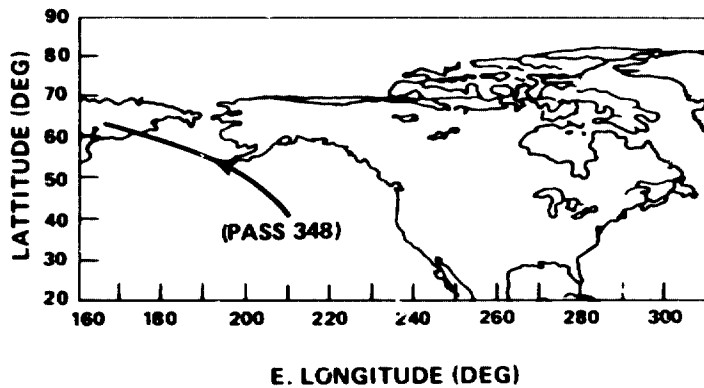


FIGURE 6(a) GEOS-3 ORBIT SUBTRACK FOR ALTIMETER PASS 348.

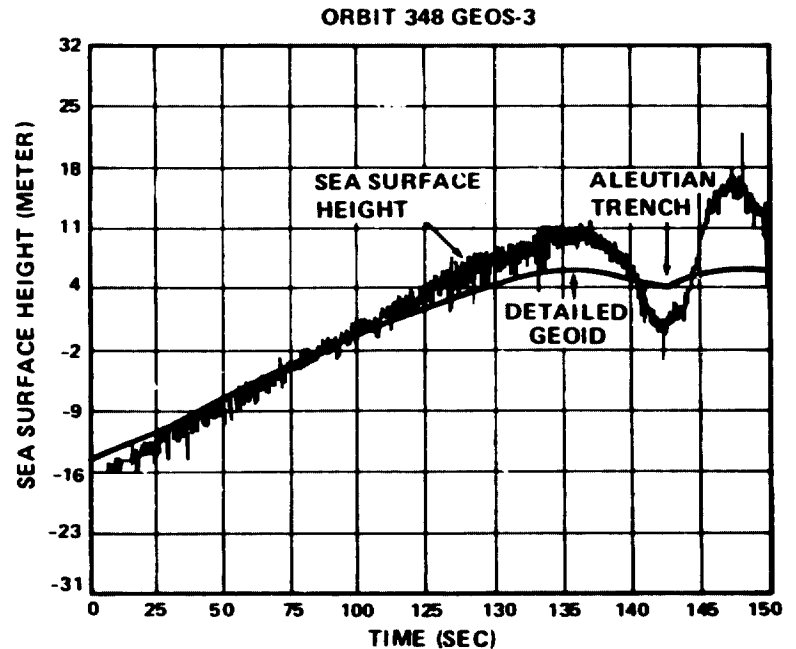


FIGURE 6(b) SEA SURFACE HEIGHT COMPARISON WITH $1^{\circ} \times 1^{\circ}$ GSFC DETAILED GEOID. TIME FROM MAY 4, 1975 13H 54M 23S.

Figure 6 GEOS-3 Sea Surface Height Profile in the Northern Pacific Area Compared with the GSFC $1^{\circ} \times 1^{\circ}$ Detailed Geoid

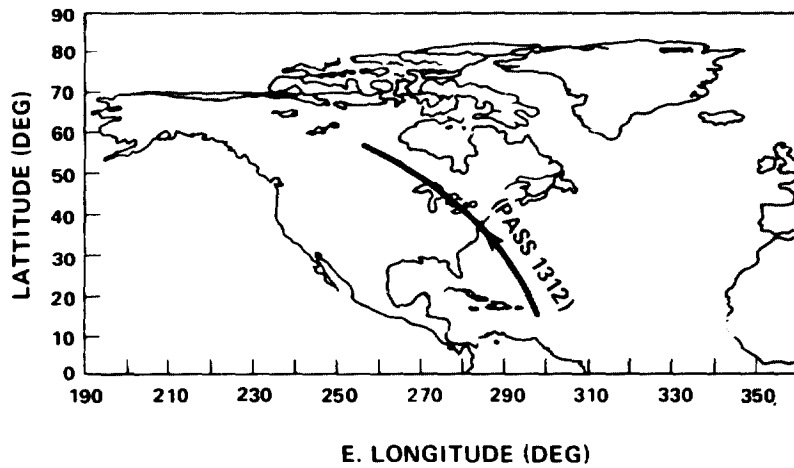


FIGURE 7(a) GEOS-3 ORBIT SURTRACK FOR ATIMETER PASS 1312.

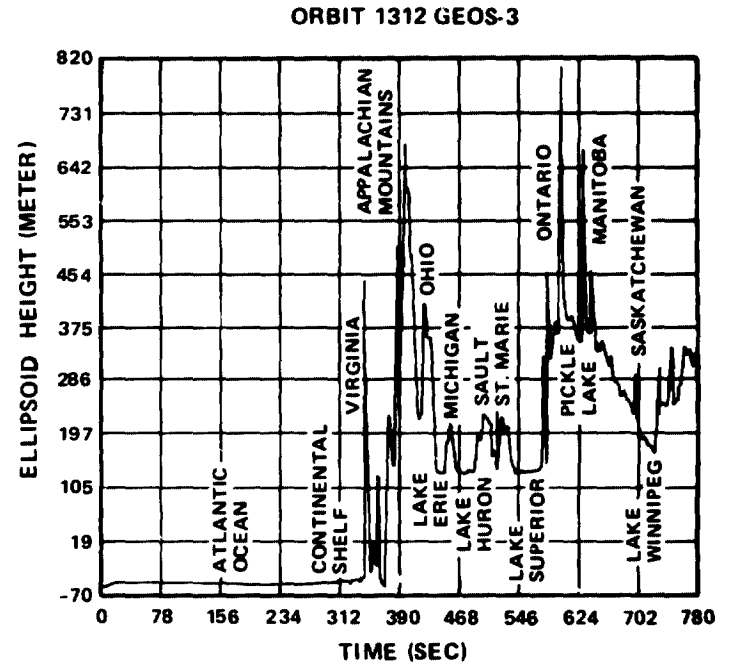


FIGURE 7(b) TIME FROM JULY 17, 1975 17H 7M 25S.

Figure 7 GEOS-3 Sea Surface Height Profile in the Western Atlantic Area and Continental United States

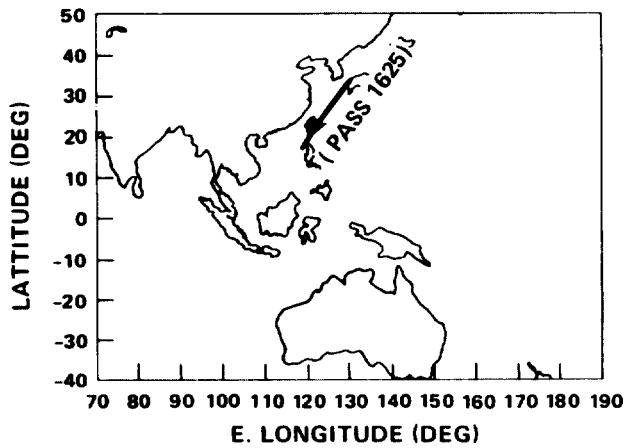


FIGURE 8(a) GEOS-3 ORBIT SUBTRACK FOR ALTIMETER PASS 1625

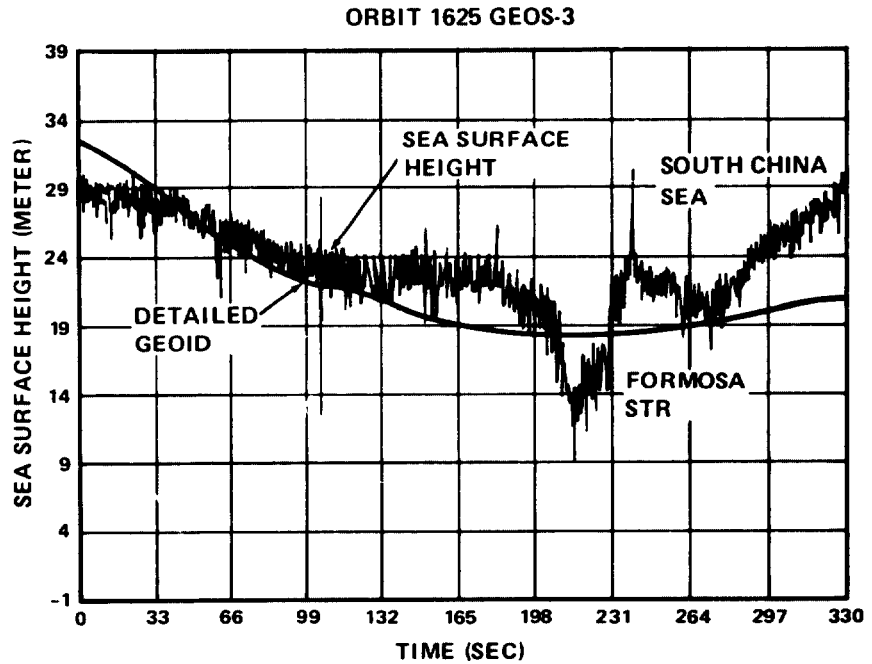


FIGURE 8(b) SEA SURFACE HEIGHT COMPARISON WITH 1°x1° GSFC DETAILED GEOID. TIME FROM AUGUST 2, 1975 20H 39M 49S

Figure 8 GEOS-3 Sea Surface Height Profile in the Formosa Strait Area Compared with the GSFC 1° x 1° Detailed Geoid